



Contents lists available at ScienceDirect

## International Journal of Machine Tools &amp; Manufacture

journal homepage: [www.elsevier.com/locate/ijmactool](http://www.elsevier.com/locate/ijmactool)

## Performance of a new segmented grinding wheel system

T. Nguyen, L.C. Zhang\*

School of Aerospace, Mechanical and Mechatronic Engineering, The University of Sydney, NSW 2006, Australia

## ARTICLE INFO

## Article history:

Received 15 August 2008

Received in revised form

21 October 2008

Accepted 30 October 2008

Available online 30 November 2008

## Keywords:

Coolant saving

Residual stress

Segmented grinding wheel

Surface integrity

## ABSTRACT

This paper investigates the mechanical and thermal effectiveness of a new segmented grinding wheel system with controlled radial coolant supply. The applicability of the system was examined in terms of grinding forces, specific energy and ground surface integrity in plunge grinding of AISI 4140 steel. It was found that compared with a standard grinding wheel, the new system enhanced the grindability with a lower specific energy and less application of coolant. It was also found that the new grinding system could effectively maintain the sharpness of active cutting edges, evidenced by the minimisation of ploughing and rubbing deformation in ground workpieces. The cleaning capacity of the wheel was improved and chip loading on wheel surfaces was avoided. Meanwhile, the new wheel system generated better surface integrity without tensile residual stresses.

Crown Copyright © 2008 Published by Elsevier Ltd. All rights reserved.

## 1. Introduction

Grinding is expensive but is vital to many precision components that require smooth surface and fine tolerance. In grinding, the specific energy consumed for a unit material removal is considerably high [1,2]. Virtually, the majority of grinding energy is converted to heat, which results in an elevation of temperature in the wheel–workpiece contact zone (grinding zone). Such excessive temperature rise under large grinding stresses accelerates the wear of grinding wheels and causes various types of thermal damages to the components subjected to grinding [3,4]. To avoid these problems, frequent dressing of wheels is often required, although this reduces the production rate significantly. On the other hand, to eliminate grinding-induced thermal damages, such as burning, detrimental residual stresses and distortion, grinding operations are usually performed at low material removal rates.

Some investigations on grinding wheel development have tried to reduce thermal damages by using superabrasives, such as CBN abrasives because of their high thermal conductivities [5]. This has led to many satisfactory results. Nevertheless, the thermal damage problem in high-speed grinding remains [1]. Diamond abrasives, in spite of their extreme hardness, are not suitable for grinding most ferrous metals because of excessive diamond wear caused by their graphitisation and carbon diffusion [6,7]. A common solution for minimising the thermal damage in grinding is to use a sea of coolant, which contains chemical additives

such as phosphorous, sulphur and chlorine compounds. Unfortunately, these additives react with the fine metallic particles from grinding and produce a noxious mixture of chemicals, including microbial organisms and their associated toxins, leading to serious occupational, health and safety issues [8,9].

Over the past decades, minimising the usage of coolant has been a focus in manufacturing research such as the new design and alignment of nozzles [10–12]. However, modern grinding techniques are mostly of high spindle speeds which usually bring about an air curtain around a rotating wheel and limit the penetration of coolant into the grinding zone. In addition, the coolant flow is often trimmed down by the spin-off and splashing of the fast spinning wheel. Attempts to solve the problem have got a limited success [13]. Another approach is to seek for a replacement of the conventional coolants, e.g., using cold air [14] or cryogenics such as liquid nitrogen [15,16]. This, again, even by ignoring the cost of cryogenics, has not been significantly effective.

The authors introduced a grinding wheel system with a segmented surface and a pressurised radial cooling mechanism [17–19]. The wheel body contains perforated holes between the segments, allowing coolant to be squeezed through to the grinding zone. In an investigation on the mechanism of coolant penetration, the authors found that using such a wheel structure, the capacity to enable the coolant to penetrate into the grinding zone increases with the wheel speed. This is different from that in a standard wheel of which the capacity decreases [18,19]. This finding promises a solution to minimise the coolant usage in grinding at high spindle speeds. However, a fair understanding is unavailable.

This paper aims to assess the thermal and mechanical effectiveness of the above segmented wheel system using the surface integrity of ground components as a criterion.

\* Corresponding author. Tel.: +61 29351 2835.

E-mail addresses: [thai.h.nguyen@gmail.com](mailto:thai.h.nguyen@gmail.com) (T. Nguyen), [lzhang@usyd.edu.au](mailto:lzhang@usyd.edu.au) (L.C. Zhang).

## 2. Experiment

Fig. 1 shows the structure of the grinding wheel-fluid chamber system. The wheel consists of 144 equally spaced CBN segments of B100P120V, assembled on a mild steel rim. The radial bore holes of 2 mm in diameter on the wheel rim between the segments enable the coolant to flow through. The wheel diameter is 300 mm. The coolant chamber is of Teflon (PTFE), which was machined to best fit to the wheel groove. There are two advantages of introducing coolant in this way. Firstly, it can force the coolant to penetrate into the grinding zone where cooling is mostly needed. Secondly, the coolant application is localised, avoiding an over flow of coolant through the entire periphery of the wheel, and hence minimises the coolant wastage. Depending on the wheel speed, the angular position of the chamber can be adjusted to ensure that the major flow of coolant is within the grinding zone (Fig. 1b). A standard grinding wheel of 300 mm in diameter, made of the same abrasive material as the segmented wheel was also used for a comparison study. Coolant was provided with a nozzle of 10 mm in diameter and was placed about 50 mm away from the grinding zone and 30° tangential to the specimen surface subjected to grinding. The flow rate was controlled by a valve.

Surface morphology of the specimens was inspected and analysed using a digital microscope, Keyence VHX-100 with a high-resolution zoom lens VH-Z50. The built-in method of depth from defocus (DFD) was used to obtain the 3D images and cross-section profiles. Instantaneous images of the coolant flow during the high-speed rotation of the wheel were recorded by the high-speed strobe photography where a stroboscope (1538-A Strobotac) of flash duration less than 3  $\mu$ s was used in synchro-

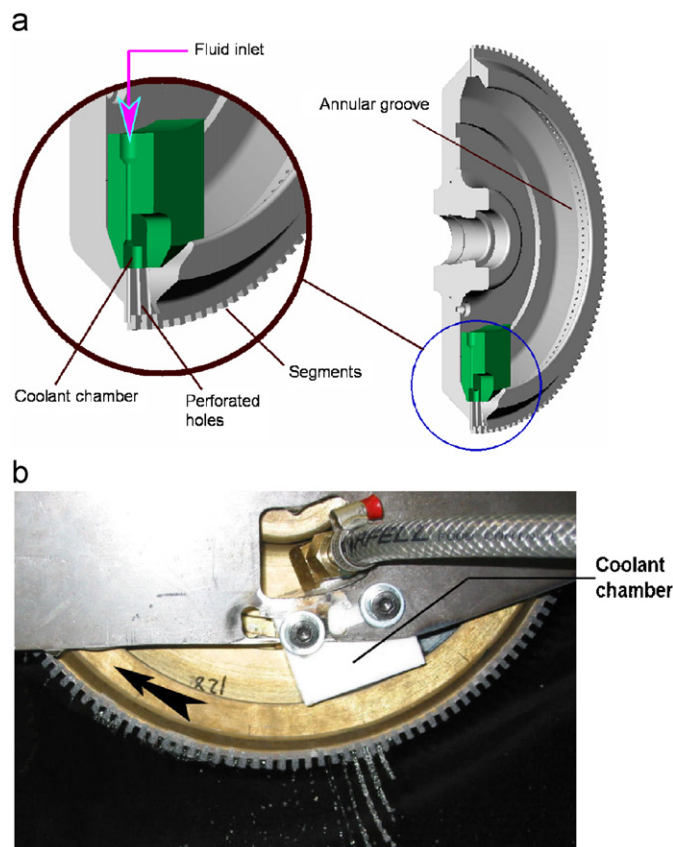


Fig. 1. The developed grinding system: (a) a cross-sectional view and (b) the wheel-coolant chamber assembly.

nisation with a camera (Nikon 35-135). Grinding forces were measured using a KISTLER dynamometer (Type 9257B). Residual stresses were measured using an MSF-3M X-ray stress analyser (Rigaku Co., Japan), using the iso-inclination method. The X-ray source was Cr K radiation generated from an X-ray tube operated at the maximum load of 30 kV and 10 mA. The angle of the X-ray incidence and reflection with respect to normal to the specimen surface were precisely measured using a goniometer (Fig. 2). The signal of the diffracted X-ray intensity obtained from the detector was transferred to a computer to compute and interpret the signal to the value of residual stress. To measure the residual stress variation in the subsurface, layers of the material need to be removed. To avoid the alteration of residual stresses by a mechanical removal process [20,21], an electro-polishing process was conducted on a Movipol-3 machine with an electrolyte solution of 82% ethanol, 8% perchloric acid ( $\text{HClO}_4$ ) 60% and 10% 2-butoxyethanol ( $\text{C}_6\text{H}_{14}\text{O}_2$ ) by volume. The thickness of the removed layer was measured by the focusing movement function of the optical microscope mentioned above. The stress relief perturbed by the electro-polishing removal was corrected by the method proposed by Moore and Evan [22]. Residual stresses were measured in the middle of the sample where the grinding conditions were the most stable; and in three directions, namely along the grinding direction ( $\sigma_{yy}$ ), perpendicular to the grinding direction ( $\sigma_{xx}$ ), and along that of 45° to the grinding direction ( $\sigma_{45}$ ). The maximum shearing stresses ( $\tau_{\max}$ ) were determined by the Mohr's circle of stresses.

Grinding experiments were conducted on a CNC surface grinder, Minini Junior 90 CNC-M286. The grinding conditions are shown in Table 1. The workpiece material was AISI 4140 steel. The specimens were cut-to-size with the ground width of 5 mm from a large block of raw material. To remove the stress introduced by specimen preparation, the specimens were annealed by heating them to above 600 °C in a vacuum furnace to prevent oxidation. Prior to actual grinding at a desired depth of cut, the annealed samples were levelled under flooding coolant, Noritake SA-02 (1:60), with several grinding passes at a small depth of cut (2  $\mu$ m). In the levelling, freshly dressed wheels were always used to ensure that the initial residual stresses on specimens were minimised. Residual stresses induced by the levelling grinding were examined by repeating the process on four samples and the results were close to zero, i.e.,  $\sigma_{xx} = -4.67 \pm 4.24$  MPa and  $\sigma_{yy} = -2.39 \pm 7.32$  MPa. Hardness of the sample was measured using a hardness tester, Shimadzu Seisakusho NT-M00.

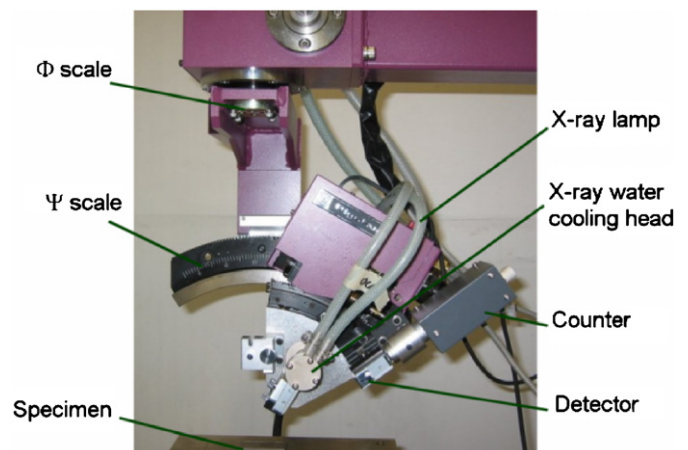


Fig. 2. Goniometer of the X-ray diffraction machine.

**Table 1**  
Grinding conditions.

Grinding machine	Minini Junior 90 CNC-M286
Workpiece	AISI 4140 (0.40%C, 0.25%Si, 0.80%Mn, 0.90%Cr and 0.20%Mo) HV <sub>(300g)</sub> = 350 ± 25
Grinding method	Horizontal plunge surface grinding in down grinding mode
Grinding speed	23 m/s
Table speed	400 mm/min
Depth of cut	10–50 μm (step 5 μm)
Dressing	<ul style="list-style-type: none"> <li>• Single-point diamond, radius = 1 mm</li> <li>• Wheel speed 1500 rpm</li> <li>• Cross feed rate 157 μm/rev</li> </ul>
Cooling	<ul style="list-style-type: none"> <li>• Water-soluble oil, Noritake SA-02 (concentration 1:60 with viscosity of <math>12.1 \times 10^{-4}</math> Pa.s)</li> <li>• Flow rate: 4.8 litres/min (saving mode) and 14.5 litres/min (high rate mode)</li> </ul>

### 3. Results and discussion

#### 3.1. Grinding forces and specific energy

Fig. 3(a) and (b) illustrate the grinding forces and specific energy, respectively, when using the standard and segmented wheels under different coolant flow rates. At the coolant saving mode, the grinding forces and specific energy were higher when using the standard wheel and the difference became more noticeable at the depth of cut above 30 μm. Below this depth of cut, which is considered to be associated with fine undeformed chip thicknesses, specific energy was significantly high under all conditions. It could be due to the size effect [1], because small pieces of material have a proportionally greater strength to cause a higher grinding energy [23,24]. At the depth of cut of 45 μm, burning with a black layer appeared on the ground surface in conjunction with very high tangential and normal grinding forces of 15.5 and 44.5 N. A higher depth of cut of 45 μm could be achieved with the standard wheel when the high rate coolant mode of 14.5 litres/min was used. However, in comparison with that obtained from the segmented wheel even with the saving coolant mode, the specific energy was higher (about 6.6–23.5%). It is clear that the use of segmented grinding wheel system enhanced the grindability even with a much less coolant application.

#### 3.2. Surface morphology

Fig. 4 illustrates the morphology of the surface ground by the standard wheel (high rate coolant mode) and segmented wheel (saving coolant mode). The material's side flows due to abrasive ploughing were obvious on the surfaces ground by the standard wheel (Fig. 4a), which did not seem to occur on those ground by the segmented wheel (Fig. 4b). The profiles of the ground surfaces in the direction perpendicular to the grinding direction, Fig. 5, show that the segmented wheel produces numerous tiny 'peaks' on the ground workpiece surfaces. It is known that a single abrasive grit takes three roles in grinding: rubbing, ploughing and cutting [1,2,4]. By rubbing, the elastic/plastic deformation occurs without a noticeable material removal. With ploughing, the material is plastically extruded in both grinding direction and in the direction transverse to it. The flow of material on the transverse direction leaves the side flows on the edges of grinding

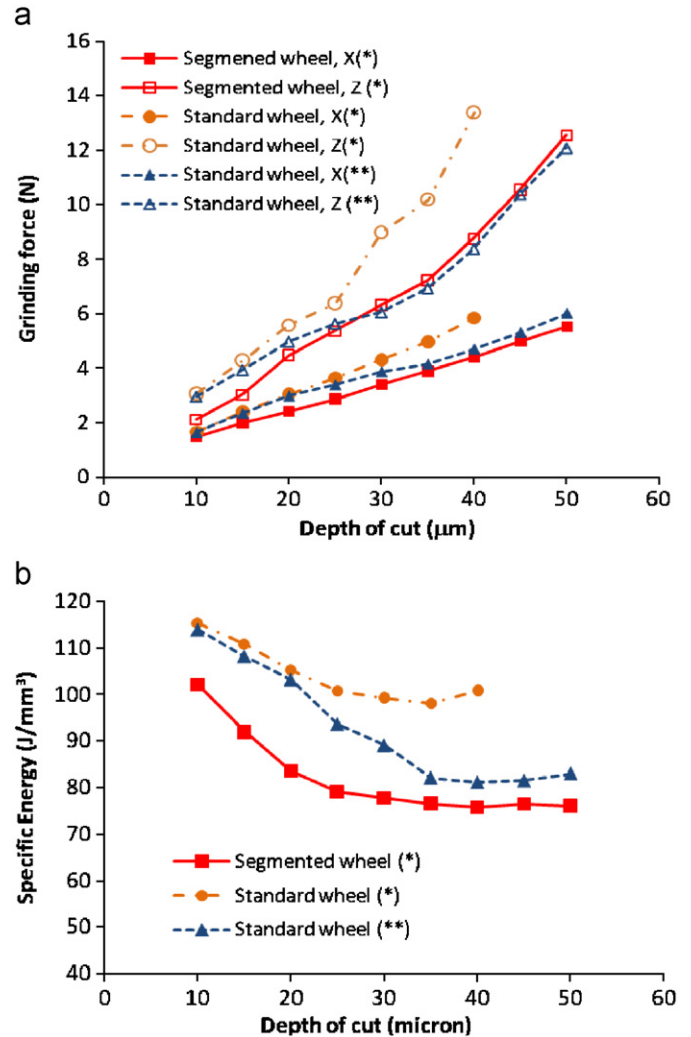


**Fig. 3.** Forces and specific energy in grinding with the segmented wheel and standard wheel systems and at different coolant flow rates of (\*) 4.8 litres/min and (\*\*) 14.5 litres/min: (a) grinding forces (X: tangential force and Z: normal force) and (b) specific energy.

grooves. Material is mainly removed by shearing via the cutting action that apparently depends on the sharpness of the abrasive cutting edges. The morphology generation of a ground surface is influenced by several factors including the characteristics of the wheel, the properties of the workpiece material, the grinder used, and the grinding conditions [2]. In the present study, the same material was ground on the same machine with nominally the same grinding conditions; thus the causes for the above morphology differences can be reasonably attributed to the wheel performance under distinguished coolant penetration mechanisms during the material removal process. Figs. 4 and 5 showed that in comparison with the standard wheel, the segmented wheel system has effectively reduced the ploughing and rubbing actions of the cutting edges because it is clear that the morphology of the ground surface mimics more the surface profiles of the cutting edges of the grinding wheel (Fig. 6).

The above result also attributes to the effective coolant flow of the segmented wheel. As well-known, the coolant plays three major roles in grinding: heat removal, lubrication and chip cleaning (prevention of the grinding wheel surface from chip loading), where chip cleaning is particularly important in fine grinding because grit spaces are small (~215 μm in the case of the

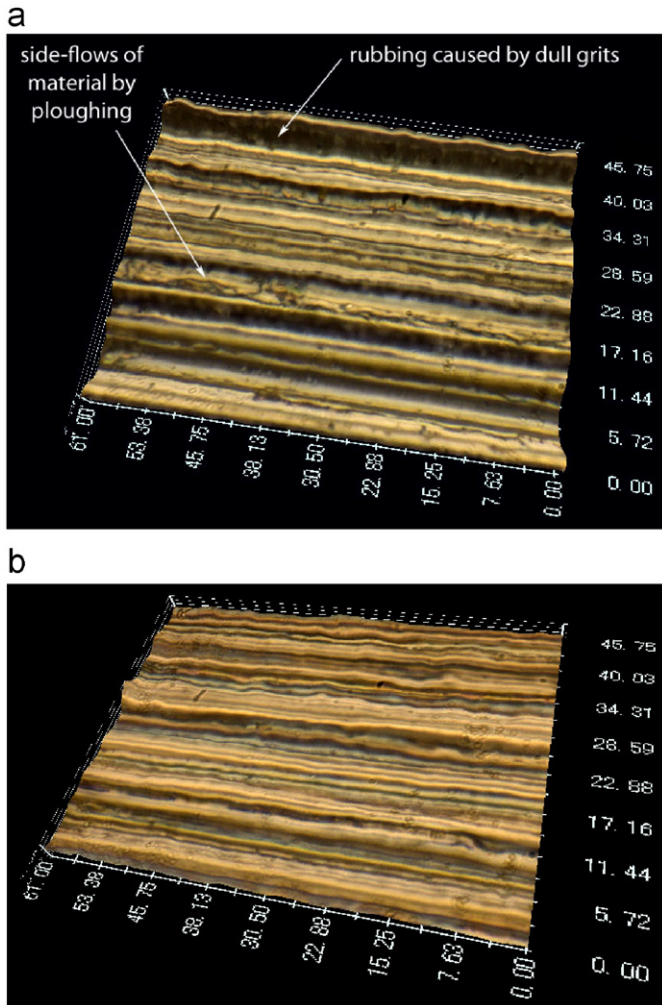


**Fig. 4.** Surface morphology of ground workpieces ground at 35  $\mu\text{m}$  depth of cut (unit is in micrometer): (a) surface generated by the standard wheel (coolant flow rate of 14.5 litres/min) and (b) surface generated by the segmented wheel (coolant flow rate of 4.8 litres/min).

present study). To achieve the cleaning, a high pressure and a large volume of coolant are often required [2,25]. When using the standard wheel, the cleaning was only active at the entrance of coolant application, as illustrated in Fig. 4a. Some chips (Fig. 7) peeled off by the coolant jet from the wheel surface might re-enter into the grinding zone. Under a high pressure within the grit spaces of the zone, these chips could plough the material and result in irregular grooves. When using the segmented wheel, as illustrated in Fig. 6b, the coolant was pumped through the channels of the wheel to enhance its penetration into the grinding zone [18], which in addition to a more effective cooling and lubrication, promoted greatly the chip cleaning and avoided the re-entrance of chips into the grinding zone. As a consequence, the sharpness of the active grits was maintained (Fig. 8).

The significance of the above result lies in the segmented grinding wheel system that allows a higher depth of cut achieved and minimises the frequency of wheel dressing and truing.

### 3.3. Subsurface characteristics

Fig. 9 shows the measured surface and subsurface residual stresses along the grinding direction  $y$  ( $\sigma_{yy}$ ), in direction  $x$ , which is perpendicular to  $y$  ( $\sigma_{xx}$ ) and in the direction of  $45^\circ$  to  $y$  ( $\sigma_{45}$ ). It can be seen that a high compressive surface stress ( $-335\text{ MPa}$ )

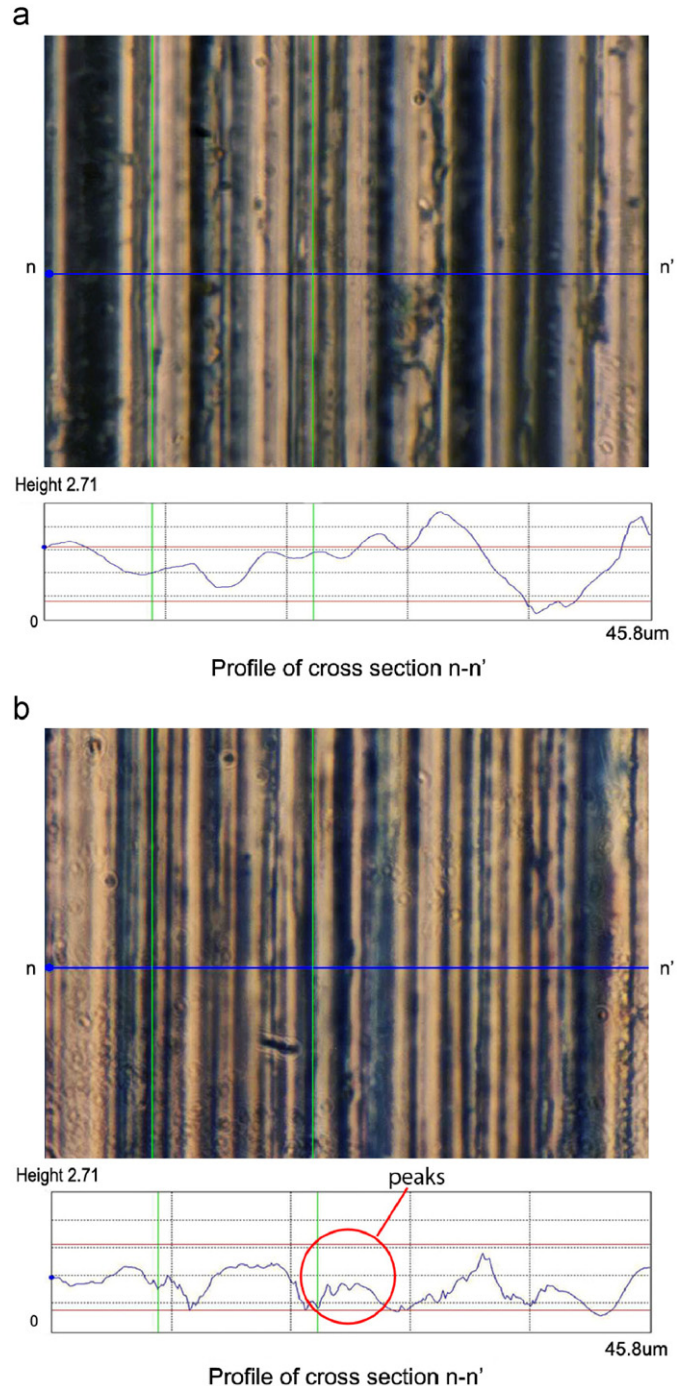


**Fig. 5.** Surface profiles of ground workpieces ground at 35  $\mu\text{m}$  depth of cut: (a) by the standard wheel (coolant flow rate of 14.5 litres/min) and (b) by the segmented wheel (coolant flow rate of 4.8 litres/min).

was induced by the standard wheel (Fig. 9a). However, this beneficial feature was not maintained in the subsurface. At a depth below 50  $\mu\text{m}$ , tensile stresses were found in the grinding direction. When using the segmented wheel system, the surface residual stress was less compressive ( $-185\text{ MPa}$ ) but the compressive nature of the stresses was maintained to a much deeper subsurface (Fig. 9b).

It is known that there are three principal sources of residual stress generation in grinding [4,21]: mechanically-induced plastic deformation, which usually leads to compressive stresses, thermal deformation, which normally produces tensile stresses, and phase transformation, which can yield either compressive or tensile

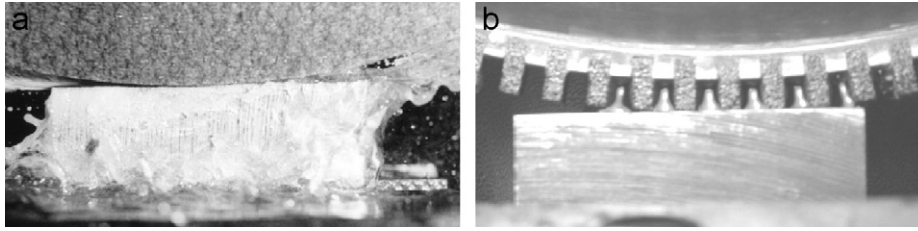


**Fig. 6.** Transportation of coolant using different grinding wheel systems, coolant flow rates: 14.5 litres/min for standard wheel and 4.8 litres/min for segmented wheel (high-speed strobe photography, wheel speed at 23 m/s and table speed at 400 mm/min): (a) the standard wheel and (b) the segmented wheel.

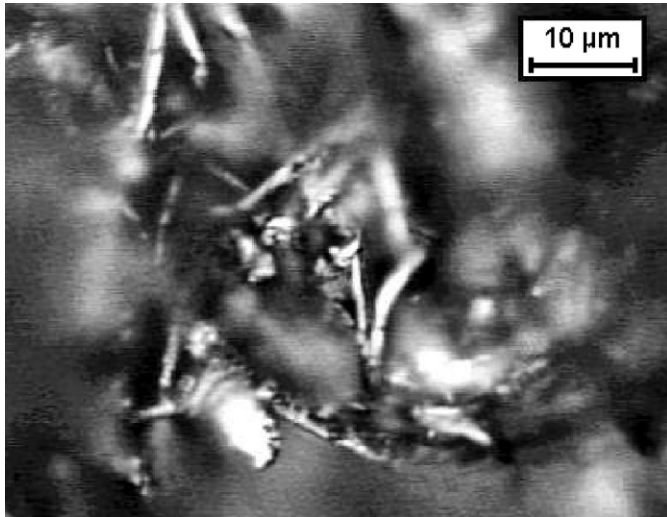


**Fig. 7.** Clogged chips collected from the standard wheel surface after grinding at 35  $\mu\text{m}$  with coolant flow rate of 14.5 litres/min.

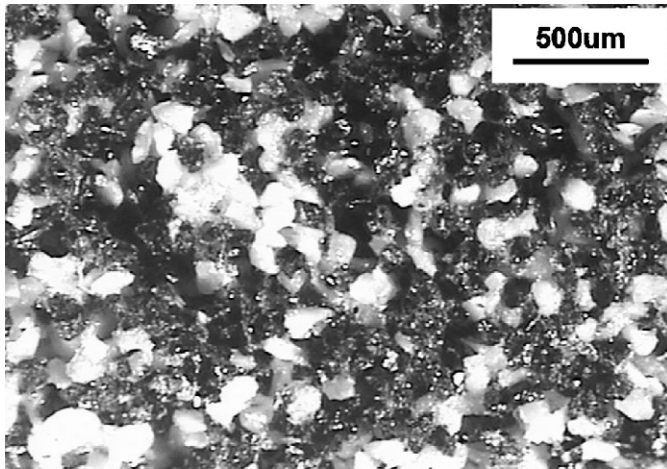


**Fig. 8.** Fresh surface of the segment after grinding at 35  $\mu\text{m}$  with coolant flow rate of 4.8 l/min.

stresses depending on the volume change of the new phase. In the present study, the surfaces hardness of the workpieces ground by the segmented and the standard wheels were found to be  $HV_{(300g)} = 375$  and  $HV_{(300g)} = 400$ , respectively. These values are slightly higher than the ones prior to grinding, which may be due to the cold hardening caused by grinding [21] but they are much lower than that of the martensite obtained by an ordinary quenching ( $HV_{(300g)} = 560$ ) [26]. This means that mechanical and thermal deformations are the sources of residual stress formation here.

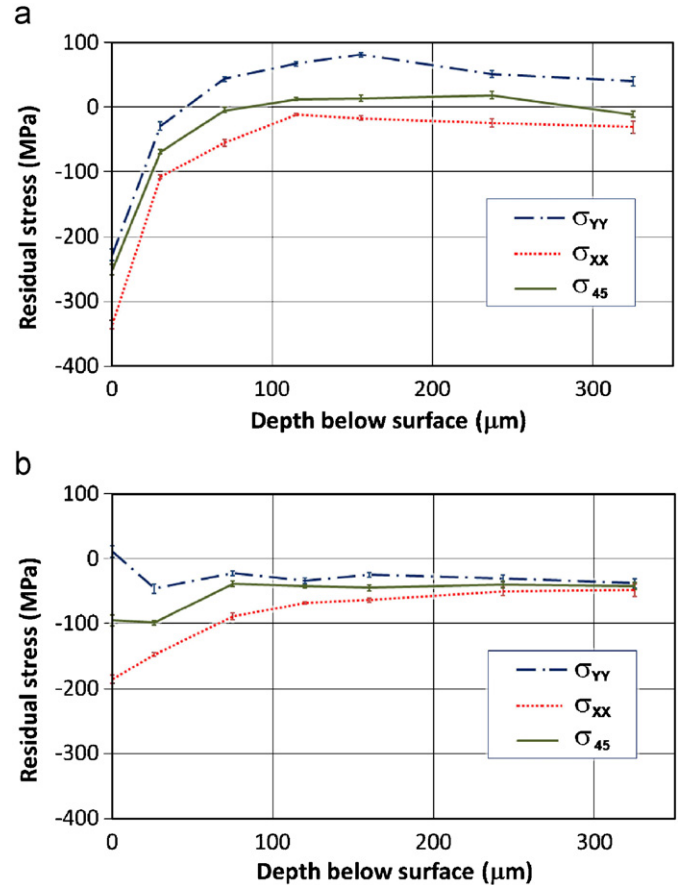


**Fig. 9.** Distributions of residual stresses produced by different grinding wheels at 35  $\mu\text{m}$  depth of cut: (a) by the standard wheel (coolant flow rate of 14.5 litres/min) and (b) by the segmented wheel (coolant flow rate of 4.8 litres/min).

As previously discussed, when grinding with the standard wheel, the workpieces experienced a great deal of rubbing and ploughing, and hence lead to large compressive residual stresses in the surface (Fig. 9b). However, the mechanical stresses are limited within a thin layer, below which the residual stresses are dominantly generated by thermal deformation and are tensile [3]. Due to the effective cooling and less ploughing and rubbing when using the segmented wheel system, it is reasonable to see that tensile stresses in this case are not noticeable (Fig. 9b).

Fig. 10 shows the variation of the maximum shear residual stresses ( $\tau_{\text{max}}$ ) with the subsurface depth. It is interesting to note that the material ground by the standard wheel appeared to have a constant magnitude of  $\tau_{\text{max}}$  close to 40 MPa. In contrast,  $\tau_{\text{max}}$  in the workpiece ground by the segmented wheel decreased quickly to nearly zero. This indirectly shows that the segmented wheel can maintain its 'sharpness' in the material removal and hence the affected zone/depth by ploughing is much shallow.

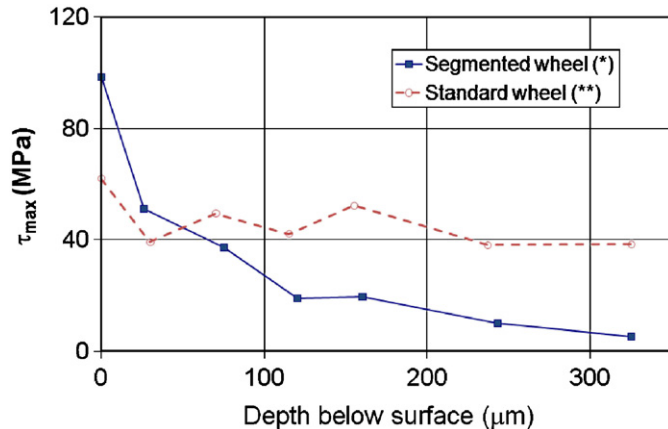


Fig. 10. Distributions of the maximum shearing stresses (depth of cut: 35 μm, coolant flow rate: (\*) 4.8 litres/min and (\*\*) 14.5 litres/min).

#### 4. Conclusions

The above discussion demonstrates that the segmented grinding wheel system has some obvious advantages in comparison with a standard wheel. It can be an economic solution for reducing environmental impact by coolant saving while providing a better surface integrity. The main conclusions on using the segmented wheel system are

- that it enhances the grindability;
- that ploughing and rubbing during the material removal are much reduced;
- that cooling to minimise thermal deformation is greatly enhanced; and
- that chip cleaning becomes efficient and hence the sharpness of the cutting edges can be maintained.

#### Acknowledgements

This project was financially supported by the Australian Research Council (ARC). The authors appreciate the permission of Associate Professor J. Wang for them to use of the digital microscope at School of Mechanical and Manufacturing, The University of New South Wales.

#### References

- [1] S. Malkin, *Grinding Technology—Theory and Applications of Machining with Abrasives*, Ellis Horwood Ltd., Chichester, UK, 1989.
- [2] M.C. Shaw, *Principles of Abrasive Processing*, Oxford University Press, Oxford, 1996.

- [3] R. Snoeys, M. Maris, J. Peters, Thermally induced damage in grinding, *Annals of the CIRP* 27 (II) (1978) 571–581.
- [4] L.C. Zhang, T. Suto, H. Noguchi, T. Waida, An overview of applied mechanics in grinding, *Manufacturing Review* 5 (4) (1992) 261–273.
- [5] S. Kohli, C. Guo, S. Malkin, Energy partition to the workpiece for grinding with aluminium oxide and CBN abrasive wheels, *Transactions of the ASME* 117 (1995) 160–168.
- [6] K.H. O'Donovan, Synthetic diamond, *Annals of the CIRP* 24 (1) (1975) 265–270.
- [7] Y. Chen, L.C. Zhang, J.A. Arsecularatne, Polishing of polycrystalline diamond by the technique of dynamic friction. Part 2: Material removal mechanism, *International Journal of Machine Tools and Manufacture* 47 (10) (2007) 1615–1624.
- [8] I.A. Greaves, Respiratory health of automobile workers exposed to metal working fluid aerosols: respiratory symptoms, *American Journal of Industrial Medicine* 32 (5) (1997) 450–459.
- [9] J. Bardin, E.A. Eisen, S.R. Woskie, R.R. Monson, T.J. Smith, P. Tolbert, K. Hammond, M. Hallock, Mortality studies of machining fluid exposure in the automobile industry: a case-control study of pancreatic cancer, *American Journal of Industrial Medicine* 32 (1997) 240–247.
- [10] R.A. Irani, R.J. Bauer, A. Warkentin, A review of cutting fluid application in the grinding process, *International Journal of Machine Tools and Manufacture* 45 (15) (2005) 1696–1705.
- [11] S. Ninomiya, M. Iwai, T. Uematsu, K. Suzuki, R. Mukai, Effect of the floating nozzle in grinding of mild steels with vitrified CBN wheel, *Key Engineering Materials* 257–258 (2004) 315–320.
- [12] S. Ebbrel, N.H. Wooley, Y.D. Tridimas, D.R. Allanson, W.B. Row, Effects of cutting fluid application methods on the grinding process, *International Journal of Machine Tools and Manufacture* 40 (2) (2000) 209–223.
- [13] T. Tawakoli, Minimum coolant lubrication in grinding, *Industrial Diamond Review* 1 (2003) 60–65.
- [14] T. Nguyen, L.C. Zhang, An assessment of the applicability of cold air-oil mist in surface grinding, *Journal of Materials Processing Technology* 140 (1–3) (2003) 224–230.
- [15] T. Nguyen, I. Zarudi, L.C. Zhang, Grinding-hardening with liquid nitrogen: mechanisms and technology, *International Journal of Machine Tools and Manufacture* 47 (1) (2007) 97–106.
- [16] S. Paul, A.B. Chattopadhyay, A study of effects of cryo-cooling in grinding, *International Journal of Machine Tools and Manufacture* 35 (1) (1995) 109–117.
- [17] T. Nguyen, L.C. Zhang, Modelling of the mist formation in a segmented grinding wheel system, *International Journal of Machine Tools and Manufacture* 45 (1) (2005) 21–28.
- [18] T. Nguyen, L.C. Zhang, The coolant penetration in grinding with segmented wheels—Part 1: Mechanism and comparison with conventional wheels, *International Journal of Machine Tools and Manufacture* 45 (12–13) (2005) 1412–1420.
- [19] T. Nguyen, L.C. Zhang, The coolant penetration in grinding with a segmented wheel—Part 2: quantitative analysis, *International Journal of Machine Tools and Manufacture* 46 (2) (2006) 114–121.
- [20] P. Prevey, Residual stress distributions produced by strain gage surface preparation, in: 1986 SEM Spring Conference on Experimental Mechanics, 1986.
- [21] H.K. Tonshoff, E. Brinksmeier, Determination of the mechanical and thermal influences on machined surfaces by microhardness and residual stress analysis, *Annals of the CIRP* 29 (2) (1980) 519–530.
- [22] M.G. Moore, W.P. Evan, Mathematical correction for stress in removed layers in X-ray diffraction residual stress analysis, *SAE Transactions* 66 (1958) 340–345.
- [23] S. Kalpakjian, *Manufacturing Process for Engineering Materials*, third ed., Addison-Wesley, Menlo Park, CA, 1997.
- [24] G. Boothroyd, A.K. Winston, *Fundamentals of Machining and Machine Tools*, second ed., Marcel Dekker Inc., New York, 1989.
- [25] O. Sinot, P. Chevrier, P. Padilla, Experimental simulation of the efficiency of high speed grinding wheel cleaning, *International Journal of Machine Tools and Manufacture* 46 (2) (2006) 170–175.
- [26] I. Zarudi, L.C. Zhang, Mechanical property improvement of quenchable steel by grinding, *Journal of Materials Science* 37 (18) (2002) 3935–3943.